

# Monte Carlo simulation of magneto-transport property in anisotropic layered structures

X. Y. Yao · Sh. Dong · J.-M. Liu

Published online: 21 August 2007  
© Springer Science + Business Media, LLC 2007

**Abstract** An anisotropic layered model structure composed of line-groups as an anisotropic bilayered manganite, is constructed based on elementary interactions in bilayered manganites. The anisotropic magneto-transport property is investigated using microscopic resistor-network scheme. The simulation reproduces qualitatively the main magneto-transport behaviors of bilayered manganites. It is shown that both the magnetic structure and the values of resistors in the resistor-network influence the electronic transport of the whole system. The resistors within the line-groups and between the line-groups play different roles in modulating the transport behaviors.

**Keywords** Ising model · Monte Carlo · Bilayer manganite

**PACS** 75.10.-b · 75.30.Kz · 75.10.Hk

## 1 Introduction

Colossal magnetoresistance (CMR) observed in the mixed-valent perovskite manganites [1] has aroused considerable interest in scientific studies and potential technological

applications. Although manganites show colossal magnetic field-induced changes in electrical resistance [1–4], the field needed is typically several Teslas, which is too large for practical technical applications. One approach to enhance the low-field magnetoresistance is to fabricate special structures [5, 6] which is composed of tunnel junctions acting as weak and field-sensitive links between two ferromagnetic manganites. In recent years, bilayer manganites which consist of such natural junction structures are gaining more and more attentions as potential low-field CMR materials.

Bilayer manganite is a member of Ruddlesden–Popper series  $([R,A]_{n+1}Mn_nO_{3n+1})$ ,  $R$  signifies rare earth and  $A$  denotes Alkaline earth) with  $n=2$ , which is composed of magnetic  $MnO_2$  bilayers and intervening rock-salt  $(R, A)_2O_2$  block [7, 8]. There are three basic exchange interactions, namely  $J_{ab}$ ,  $J_c$  and  $J'$  standing for the in-plane, inter-single-layer, and inter-bilayer exchange interactions, respectively ( $|J_{ab}| > |J_c| \gg |J'|$ ) [7]. This layered anisotropic structure shows rich physical phenomena, such as enhanced MR effects, anisotropic carrier transport, and two types of ferromagnetic ordering [7–10].

While a lot of simulations have been done about  $ABO_3$  perovskite manganites, little have been performed on the transport property of bilayer manganites. In this paper we start from a simple Ising-like model to study the transport anisotropy in a layered model structure using Monte Carlo simulation and resistor-network method. In reality, the bilayer manganites are far more complicated than our present Ising model, but we expect that the transport properties and microscopic images as evaluated from the present investigation will shed some light on the understandings of the fundamental physics of bilayer manganites.

---

X. Y. Yao · S. Dong · J.-M. Liu (✉)  
Nanjing National Laboratory of Microstructures,  
Nanjing University,  
Nanjing 210093, China  
e-mail: liujm@nju.edu.cn

X. Y. Yao · S. Dong · J.-M. Liu  
International Center for Materials Physics,  
Chinese Academy of Sciences,  
Shenyang, China

## 2 Model and simulation

We consider a two-dimensional (2D) anisotropic lattice and study its transport properties by Monte Carlo simulation (see [11]). The simulation starts from an  $L \times L$  ( $L=100$ ) Ising lattice with periodic boundary conditions applied. Imitating the bilayer structure we assume that two neighboring lines form a “line-group” ( $a$ -axis along the line-group and  $c$ -axis perpendicular to the line-group). A line-group corresponds to one  $\text{MnO}_2$  bilayer in bilayer manganites, and a single line in the line-group corresponds to a single layer in  $\text{MnO}_2$  bilayer. In order to comprehend the anisotropy in relatively simple framework, only the three most elementary interactions are considered, namely  $J_1, J_2$  and  $J_3$ .  $J_1$  denotes the exchange interaction between the two nearest neighboring spins within a line.  $J_2$  signifies the interaction between two most adjacent spins, which lie on two lines in a line-group. And  $J_3$  means the interaction between the nearest two neighboring spins lie on two adjoined line-groups.  $J_1, J_2$  and  $J_3$  correspond to  $J_{ab}, J_c$  and  $J'$  in bilayer manganites [7], so  $J_1 > J_2 \gg J_3$  should be satisfied. Due to the different interactions, the two lines in a line-group have different Hamiltonians. With regard to the odd-numbered lines and even-numbered lines, the Hamiltonians are expressed as  $H_{1i}$  and  $H_{2i}$ , respectively.  $H_{1i}$  and  $H_{2i}$  have the following forms:

$$H_{1i} = \sum_j [-J_1(S_{i,j-1} + S_{i,j+1})S_{i,j} - J_2S_{i+1,j}S_{i,j} - J_3S_{i-1,j}S_{i,j}] \tag{1}$$

$$H_{2i} = \sum_j [-J_1(S_{i,j-1} + S_{i,j+1})S_{i,j} - J_2S_{i-1,j}S_{i,j} - J_3S_{i+1,j}S_{i,j}] \tag{2}$$

where  $S_{i,j} = \pm 1$  represents the  $j$ th spin of the  $i$ th line. In addition, an antiferromagnetic interaction ( $J_{AF}$ ) is considered between the two next-nearest neighboring spins. Then the complete Hamiltonian can be written as:

$$H = \sum_{\text{odd}} H_{1i} + \sum_{\text{even}} H_{2i} + J_{AF} \sum_{[m,n]} S_m S_n - h \sum_m S_m \tag{3}$$

where  $h$  stands for the external magnetic field, and [...] means summation over the next-nearest spin pairs.

The simulation is performed in the following procedure. The standard Metropolis algorithm is employed for the lattice to reach the equilibrium configuration from an initial state with all the spins being 1. The system is believed to reach equilibrium after 50,000 MC steps and then once per 1,000 MC steps a new spin configuration is obtained. Upon the configuration the magnetization ( $M$ ) is obtained by summing up all the spins in the system, the system

resistivity is calculated by the method of resistor-network described below. About 30 results are averaged. The final results are obtained by averaging more than ten independent data with different seeds for random number generation. For convenience,  $k_B$  and the absolute value of a spin are chosen to be 1, and  $J_1, J_2, J_3$ , and  $J_{AF}$  are measured in such simplified units. The simulation is performed for the case of  $h=0$ . Through adjusting  $J_1, J_2, J_3$ , and  $J_{AF}$ , the simulated temperature is adjusted to be very close to the experiment in unit of K, so we can compare our simulation results with experimental data.

## 3 Discussion about resistor-network

In our simulation a resistor-network is constructed based on the spin configuration that was obtained from simulation (see [11]). The lattice resistivity is calculated using the method from [12]. Owing to the anisotropy of our model, the resistivity is orientation-dependent, namely  $\rho_{ab}$  refers to the resistivity with electric current parallel to the line-group, and  $\rho_c$  for the resistivity when electric current is perpendicular to the line-group. Owing to the existence of an insulating layer between the bilayers, it is more difficult for electron to transfer between bilayers than moving within a bilayer. Accordingly, the resistors in the line-groups and between the line-groups should have different values. All resistors can be divided into four sorts, namely “metallic resistors TYPE 1” (the metallic resistors in the line-groups), “insulating resistors TYPE 1” (the insulating resistors in the line-groups), “metallic resistors TYPE 2” (the metallic resistors between the line-groups), and “insulating resistors TYPE 2” (the insulating resistors between the line-groups). Their values are defined by  $\rho_{M1}(T), \rho_{I1}(T), \rho_{M2}(T)$  and  $\rho_{I2}(T)$ , respectively:

$$\rho_{M1}(T) = A_1 + B_1 T^2 \tag{4}$$

$$\rho_{M2}(T) = A_2 + B_2 T^2 \tag{5}$$

$$\rho_{I1}(T) = C_1 e^{(T_{01}/T)^{1/4}} \tag{6}$$

$$\rho_{I2}(T) = C_2 e^{(T_{02}/T)^{1/4}} \tag{7}$$

where  $\rho_{M1}(T)$  and  $\rho_{M2}(T)$  are metallic resistivities consisting of the zero-point resistivity and electron–electron scattering ( $T^2$ ) component.  $\rho_{I1}(T)$  and  $\rho_{I2}(T)$  are the insulating resistivities in the form of Mott’s VRH model [13], which has given a satisfactory fit to experimental data above the M-I transition point  $T_c$  in a number of relevant experiments [9, 10]. All the resistivity values have the same unit of  $\text{m}\Omega \cdot \text{cm}$ .

### 3.1 Anisotropic transport behaviors

Owing to the insulating layer between the bilayers, we choose appropriate parameters to make  $\rho_{12}(T)$  higher than  $\rho_{11}(T)$  above  $T_c$ . Below  $T_c$  the whole system is transformed into ferromagnetic metal,  $\rho_{11}(T)$  and  $\rho_{12}(T)$  do not affect the system’s resistivities. For simplicity, we assume that  $\rho_{M1}(T)$  is identical to  $\rho_{M2}(T)$ , defined as  $\rho_M(T)$ . Metallic resistors TYPE 1 together with TYPE 2 are named ‘metallic resistors’. The detailed forms of  $\rho_{12}(T)$ ,  $\rho_{11}(T)$  and  $\rho_M(T)$  are:

$$\rho_M(T) = 0.157576 + 0.157576 \times 10^{-3} T^2 \tag{8}$$

$$\rho_{I1}(T) = 2.44243 \times 10^{-11} e^{(2.1 \times 10^8 / T)^{1/4}} \tag{9}$$

$$\rho_{I2}(T) = 3.09972 e^{(2.0 \times 10^6 / T)^{1/4}} \tag{10}$$

Taking  $J_1=185$ ,  $J_2=135$ ,  $J_3=0.1$ , and  $J_{AF}=1.25$ , we performed extensive simulations on the anisotropic transport behaviors of the layered structure. The simulated resistivities as functions of  $T$  are shown in Fig. 1 by the open squares and circles. For reference the pioneer experimental work of Kimura et al. [8] is also presented by solid and dash lines. It is clearly shown that the in-plane resistivity  $\rho_{ab}$  exhibits a broad maximum at  $\sim 270$  K, which indicates the in-plane two-dimensional ferromagnetic short-range spin ordering. For resistivity  $\rho_c$  perpendicular to the  $\text{MnO}_2$  bilayers, which is much higher than  $\rho_{ab}$ , a sharp peak at  $\sim 100$  K is observed. This behavior is related to the three-dimensional ferromagnetic spin ordering. Our simulation results are qualitatively similar to the experimental data. The peak of  $\rho_{ab}$  implies in-line one-

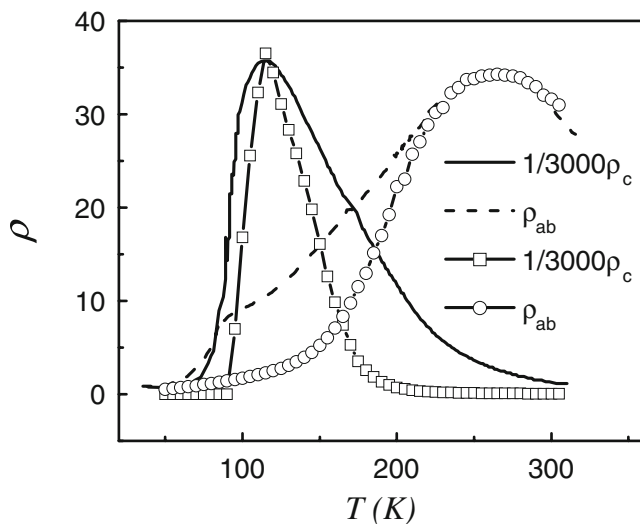


**Fig. 1** Simulated curves of the resistivities ( $1/3,000\rho_c$  and  $\rho_{ab}$ ) as functions of  $T$  denoted by open squares and circles, respectively. The experimental resistivity curves ( $1/3,000\rho_c$  and  $\rho_{ab}$ ) represented by solid line and dash line are taken from Kimura et al. [8]

dimensional short-range spin ordering, and the long-range spin ordering of the whole lattice leads to the steep decline of  $\rho_c$ .

The changes of magnetic structure have strong effect on the transport property of the system. Even if the systems possess the same magnetic structure, their transport properties can be different. This distinction originates from the intrinsic characteristic of the material. In our simulations, different resistivities of resistors reflect the intrinsic difference of different materials. By investigating different roles of resistors we hope to gain further comprehension on the anisotropic transport property in bilayer structure.

### 3.2 Roles of $\rho_{11}(T)$ and $\rho_{12}(T)$

Owing to the anisotropic resistor-network resulting from the anisotropic magnetic structure, the roles of  $\rho_{12}(T)$  and  $\rho_{11}(T)$  are different from each other, as shown in Fig. 2. While

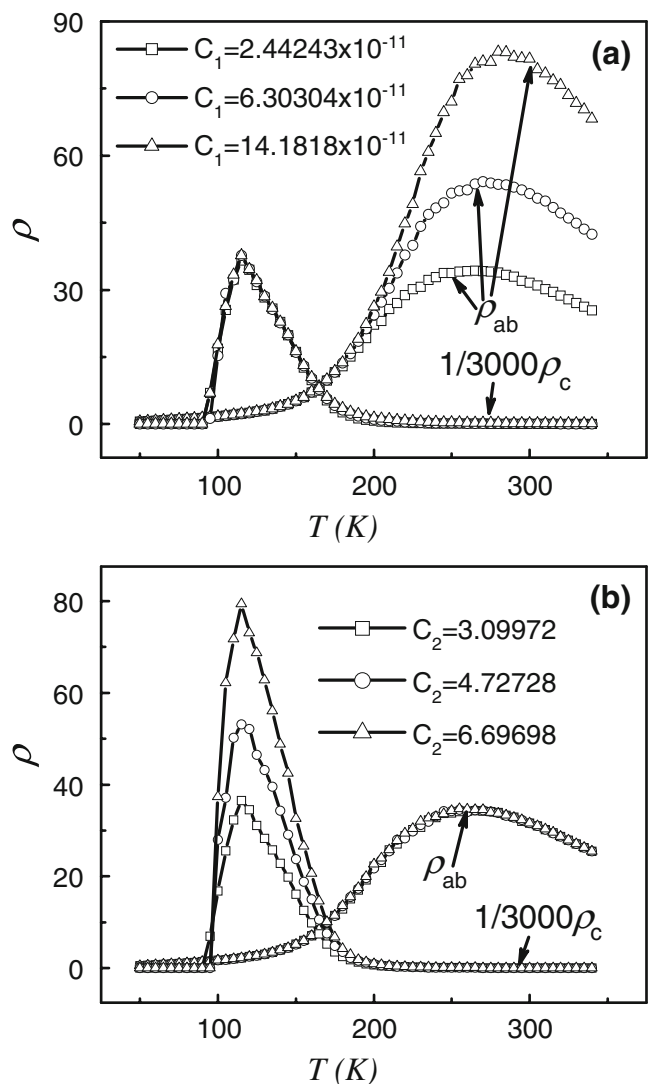
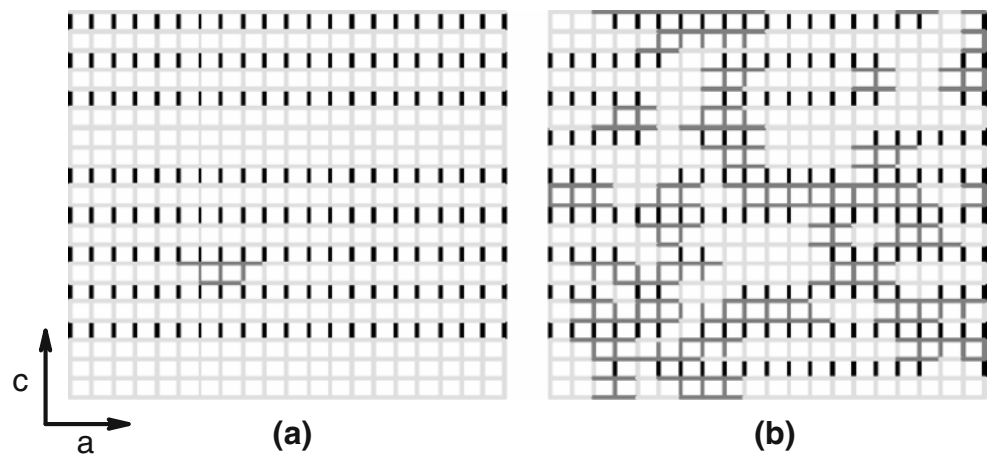


**Fig. 2**  $\rho_{ab}$  and  $1/3,000\rho_c$  as functions of  $T$  (a) for different  $C_1$ , and (b) for different  $C_2$

**Fig. 3** Snapshoted partial configurations of the resistor-network (a) at 120 K, and (b) at 270 K. The *light gray bars* indicate metallic resistor of  $\rho_M(T)$ , the *deep gray* ones denote insulating resistors TYPE 1 of  $\rho_{11}(T)$ , and the *black* ones represents insulating resistors TYPE 2 of  $\rho_{12}(T)$



keeping other parameters unchanged, Fig. 2(a) presents the results obtained by changing  $C_1$  of  $\rho_{11}(T)$ , from which we find that the  $\rho_{ab}$  peak is raised and its position moves to higher  $T$  value with increasing  $C_1$ , but no significant  $C_1$ -dependence of  $\rho_c$  is observed. The results for different  $C_2$  of  $\rho_{12}(T)$  are plotted in Fig. 2(b). It can be seen that  $\rho_c(T)$  is significantly enhanced with increasing  $C_2$  but  $\rho_{ab}(T)$  is little affected. This can be understood from the configuration of the resistor-network. Figure 3(a) and (b) give two snapshots of the configuration at 120 and 270 K, respectively. It is shown that the resistor-network at low  $T$  is comparatively regular, there are mostly metallic resistors in the line-groups and insulating resistors TYPE 2 between the line-groups, so  $\rho_c$  is strongly related to  $\rho_{12}(T)$ . The change of  $\rho_{11}(T)$  hardly influences the resistivity of the system because only very small regions of insulating resistors TYPE 1 exist at low  $T$ . At high  $T$ , the ordering of the network is broken, and blocks of insulating resistors exist here and there. Because the amount of insulating resistors TYPE 1 increases with increasing  $T$ ,  $\rho_{ab}$  will change a lot with changing  $\rho_{11}(T)$ . But the change of  $\rho_{12}(T)$  can't affect  $\rho_{ab}$  in this temperature range.

### 3.3 Effect of $\rho_{M2}(T)$

When  $\rho_{M2}(T)$  is different from  $\rho_{M1}(T)$ , the effect of  $\rho_{M2}(T)$  should be considered. Keeping other parameters unchanged,  $\rho_{M2}(T)$  takes the following form:

$$\rho_{M2}(T) = D \times \rho_{M1}(T) \tag{11}$$

The simulated resistivities as functions of  $T$  are presented in Fig. 4 for  $D=1, 10$  and  $20$ . Increasing  $D$  results in a shift of  $\rho_{ab}(T)$  upward and leftward. But little change in  $\rho_c$  is observed. The reason is that as  $T$  is close to the peak of  $\rho_c$ ,  $\rho_{M2}(T)$  is much lower than  $\rho_{12}(T)$  and the volume fraction of metallic resistors TYPE 2 is small, noting that  $\rho_c$  is mainly ascribed to  $\rho_{12}(T)$ . But for the peak of  $\rho_{ab}$ , the structure of resistor-network is irregular in that  $T$  range.

Although metallic resistors TYPE 2 are not in the line-groups,  $\rho_{M2}(T)$  also has influence upon  $\rho_{ab}$ .

## 4 Conclusion

In summary, an anisotropic layered structure is constructed based on Ising model as an approach to make realistic bilayered manganites. Its transport properties have been investigated by Monte Carlo simulations and the resistor-network method. The results show that the anisotropy of the transport behaviors is strong. The  $c$ -axis resistivity presents a sharp peak at low temperature but the  $a$ -axis resistivity demonstrates a broad M-I transition at relatively high temperature, which is qualitatively similar to the experimental results. It has been argued that not only the magnetic anisotropy resulting from anisotropic interactions contributes to the transport anisotropy, but also the value of resistors in the resistor-network can affect the transport behavior of the

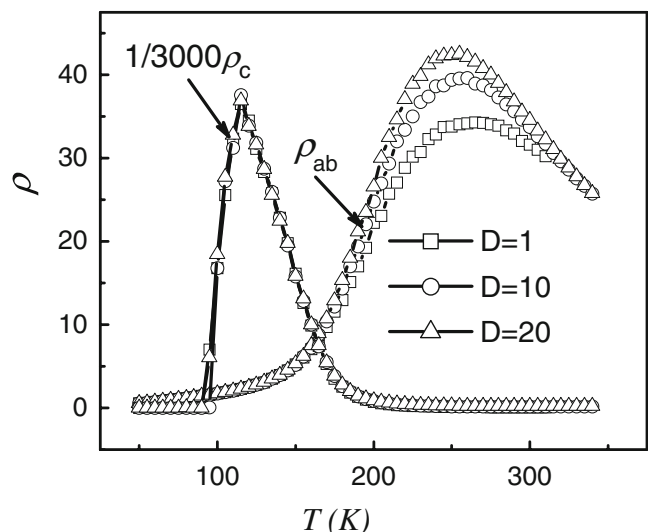


**Fig. 4**  $\rho_{ab}$  and  $1/3,000\rho_c$  as functions of  $T$  for different  $D$

system. The resistors in the line-groups and between the line-groups play different roles for the transport behavior of the system.

**Acknowledgement** The authors thank the Natural Science Foundation of China (50332020, 10021001) and National Key Projects for Basic Research of China (2002CB613303, 2004CB619004).

## References

1. S. Jin, T.H. Tiefel, M. McCormack, R.A. Fastnacht, R. Ramesh, L.H. Chen, *Science* **264**, 413 (1994)
2. R.V. Helmolt, J. Wecker, B. Holzapfel, L. Schulz, K. Samwer, *Phys. Rev. Lett.* **71**, 2331 (1993)
3. K. Chahara, T. Ohno, M. Kasai, Y. Kozono, *Appl. Phys. Lett.* **63**, 1990 (1993)
4. A. Urushibara, Y. Moritomo, T. Arima, A. Asamitsu, G. Gido, Y. Tokura, *Phys. Rev. B* **51**, 14103 (1995)
5. Y. Lu, X.W. Li, G.Q. Gong, G. Xiao, A. Gupta, P. Lecoeur, J.Z. Sun, Y.Y. Wang, V.P. Dravid, *Phys. Rev. B* **54**, R8357 (1996)
6. J.Z. Sun, W.J. Gallagher, P.R. Duncombe, L. Krusin-Elbaum, R.A. Altman, A. Gupta, Y. Lu, G.Q. Gong, G. Xiao, *Appl. Phys. Lett.* **69**, 3266 (1996)
7. T. Kimura, Y. Tokura, *Annu. Rev. Mater. Sci.* **30**, 451 (2000)
8. T. Kimura, Y. Tomioka, H. Kuwahara, A. Asamitsu, M. Tamura, Y. Tokura, *Science* **274**, 1698 (1996)
9. H. Zhu, X.M. Liu, K.Q. Ruan, Y.H. Zhang, *Phys. Rev. B* **65**, 104424 (2002)
10. H. Zhu, X.J. Xu, L. Pi, Y.H. Zhang, *Phys. Rev. B* **62**, 6754 (2000)
11. X.Y. Yao, S. Dong, H. Zhu, H. Yu, J.-M. Liu, *J. Appl. Phys.* **98**, 093908 (2005)
12. D.J. Frank, C.J. Lobb, *Phys. Rev. B* **37**, 302 (1988)
13. M. Viret, L. Ranno, J.M.D. Coey, *Phys. Rev. B* **55**, 8067 (1997)